Dimensionality and size effects in simple metals

Inder P. Batra,* S. Ciraci,† and G. P. Srivastava‡
IBM Zurich Research Laboratory, 8803 Rüschlikon, Switzerland

J. S. Nelson§ and C. Y. Fong§
IBM Almaden Research Center, Mail Stop K33/801, 650 Harry Road, San Jose, California 95120-6099
(Received 19 June 1986)

A detailed discussion of quantum-size effects and the dimensionality in simple (*s-p* bonded) metals is presented by using aluminum as a prototype. The density of states, work function, surface energy, surface relaxation, and subband energies are calculated for films of varying thicknesses. Oscillatory variations of various physical properties correlate well with the surface charge density which itself varies with the film thickness. All calculations are performed using the self-consistent pseudopotential method and the planarly averaged one-dimensional potential generated from it. Total-energy calculations and forces on various atomic planes lead to important conclusions about surface relaxation.

I. INTRODUCTION

During the last decade, extensive research has been carried out on various physical and chemical phenomena of metal surfaces. On the theoretical side, several methods to calculate the electronic structure and energetics of systems with two-dimensional (2D) periodicity have been developed, and used to investigate surface geometry, intrinsic and adatom-induced surface states of metals. Specifically, such ground-state properties as surface energies, work functions, and electronic charge densities can now be calculated from first principles and are usually in reasonable agreement with experimental data.[1] These studies have helped in understanding the data obtained by advanced and ingenious experimental techniques. And yet, only a few of these reports mainly focussing on the properties of semi-infinite metals pointed out that the size (thickness) of the metal becomes important when the film is very thin: For example, in a thin Pb film the electron standing-wave states could be observed by electron tunneling;[2] oscillations of the chemical potential due to the thickness were found to influence the width of the superconducting gap of the metal film,[3] and calculations for a copper monolayer predicted striking changes from bulk behavior.[4] Recently, it has also been shown that localization effects can be significantly enhanced when the size of an Au film varies.[5]

Advances made in growth techniques now enable control of the thickness of metal films deposited on various substrates in the monolayer range, and measurement of their exotic structures and remarkable properties. It has recently been proposed that the mechanism pinning the Fermi level (and hence the height of the Schottky barrier) changes with the thickness of the metal film deposited on a covalent semiconductor.[6] Also, novel superconductive properties of the Ag monolayer adsorbed on the Ge surface have been reported.[7] All these findings exemplify the unusual behavior of thin metal films which are rather different from bulk or semi-infinite metals. In the latter, the one-electron states may be described by three-dimensional (3D) propagating Bloch states and evanescent waves localized in the surface region.[1] However, for thin films this description of one-electron states may not be adequate. As a matter of fact, electrons confined in thin films have a quantization of states quite different from the bulk, and also from the semi-infinite metal. The more appropriate description is provided by standing waves, and the energy-level spectrum splits into subbands.[8,9] The unusual behavior of metal films, as evidenced by a few examples mentioned above, is connected with a different quantization of states upon lowering their dimensionality, and is known as the quantum size effect (QSE).

Early studies[10–12] were mainly concerned with fluctuations of chemical potentials and treated the metal film within the Sommerfeld model, i.e., noninteracting electrons confined to a one-dimensional (1D) square-cut potential. Apart from these oversimplified models, Schulte[13] investigated metal films within the jellium approximation. Using the density functional theory,[14] he calculated the electronic properties of metal with varying thickness, and pointed out oscillations in the work function as a function of the slab thickness. The discrete lattice effects were considered in a detailed self-consistent-field (SCF) linear-combination-of-atomic-orbitals (LCAO's) calculation[15] confirming that the work function and the surface energy of Al and Mg films exhibit oscillatory behavior. Recently, Ciraci and Batra[16] have pointed out interesting quasi-two-dimensional features, and other effects of lower dimensionality.

In this work, we present an extensive discussion of the properties of metal films with emphasis on QSE's. Our results are based mainly on SCF pseudopotential calculations of thin Al(111) slabs, and may be generalized to simple *sp*-bonded metal films. In addition, we generate a planarly averaged 1D quantum-well potential $V(z)$ from the SCF slab potential. This potential contains discrete-lattice effects to some extent, but is simple enough to reveal fundamental aspects of systems of lower dimen-

sionality. We then assume free-electron behavior in the two remaining dimensions (xy), and solve the 1D Schrödinger equation numerically along the z axis to obtain the electronic structure of a quasi-two-dimensional system. By comparing results from the SCF slab and the quantum well, we can deduce important features regarding the quasi-two-dimensional character and dimensionality of the metal films. The variations of several physical properties as a function of thickness such as bandwidth, work function, surface energy, subband energies, charge density, and surface relaxations, are analyzed. It is shown that the size effects are not only limited to the work function and surface energy, but also manifest themselves in many other properties. The density of states at the Fermi-level changes in quantized steps as a function of the film thickness leading to oscillatory behavior of the electronic properties. The form of the state distribution provides a criterion for the dimensionality of the system. By calculating forces acting on the atoms in the ideal configuration, it is found that thin films of sp bonded metals are subject to both lateral and oscillatory multilayer vertical relaxations. The sign of the forces acting on the subsurface layer changes as the thickness is varied. More importantly, the force exerted on the topmost layer is directed inwards, but decreases as the film becomes thicker. The interlayer spacing between the surface and subsurface layer decreases in three- and five-layer slabs, but starts to increase in seven-layer-thick films. This indicates an oscillatory relaxation even for the interlayer spacings.

This novel result is expected to reconcile contrasting results, both experimental and theoretical, on the relaxation of the Al(111) surface. Previous slab calculations[17–20] have mainly been concerned with the surface states and chemisorption aspects. The present study is directed towards a new and rapidly developing area of physics; namely, systems of lower dimensionality, and is organized as follows. In the next section, the model and parameters underlying the SCF-pseudopotential and 1D calculations are briefly described. Expressions for the forces acting on the atoms are derived from the expectation values of the force operator defined within the density functional formalism. In Sec. III, calculated energy band structures, state densities, work function, and surface energies of Al(111) films of various thicknesses are presented using the theory developed for the quasi-two-dimensional systems. In Sec. IV, the analysis of charge density is given by using charge-density contour plots, and lateral and multilayer relaxations are discussed and compared with previous experimental and theoretical studies in Sec. V. Finally, in Sec. VI results are analyzed in view of the quantum-size effect and the dimensionality of the electron system. Concluding remarks are also presented in this section.

II. METHOD OF CALCULATIONS

A. SCF calculations

We performed self-consistent pseudopotential[21,22] calculations within the framework of the local-density functional theory,[14] applied in momentum space formalism.[23,24] We used nonlocal, norm-conserving ionic pseudopotentials given by Bachelet *et al.*,[25] and Ceperly-Alder exchange and correlation potentials[26] as parametrized by Perdew and Zunger.[27] Using a repeated slab geometry, calculations were carried out for one-, three-, five-, and seven-layer Al(111) films with an interslab distance of ~ 18 a.u. (equivalent to ~ 5 interlayer spacings). These films have C_{3v} point group symmetry with an inversion center at the central plane of the slab. The z axis is taken along the surface normal, so the (111) planes are parallel to the (xy) plane.

A crucial parameter in these calculations is the number of plane waves used to represent each Bloch state. This was chosen by fixing the minimum ($G^2_{\min}$) and maximum ($G^2_{\max}$) kinetic energy. Plane waves with kinetic energy $|\mathbf{k}+\mathbf{G}|^2$ less than $G^2_{\min}$ are treated exactly, and those having energy between $G^2_{\min}$ and $G^2_{\max}$ are included via Löwdin's perturbation scheme. Another important parameter, especially for a metal, is the number of $\mathbf{k}$ points in the surface Brillouin zone (BZ), where the charge density is sampled during self-consistency. The convergence with respect to these parameters becomes essential when the total energies of systems with similar structures are compared. To determine parameters suitable for our study, we carried out the total-energy calculations of the bulk Al with different $G_{\min}$, $G_{\max}$, and sampling grid.[28] In view of the results summarized in Table I, we chose $G^2_{\min}=7$ Ry, and $G^2_{\max}=9$ Ry. Within these limits, the slab Bloch states are expanded in about 540 plane waves. During the self-consistency iterations, the charge density was sampled at 49 $\mathbf{k}$ points in the surface BZ, and the Fermi level determined by the thermally broadened Fermi-Dirac distributions with $k_B T \cong 10^{-4}$ Ry.

TABLE I. Total energy E_T (Ry) and bandwidth E_W (eV) of bulk aluminum as a function of the number of $\mathbf{k}$ points in the Brillouin zone, and $G^2_{\min}, G^2_{\max}$. The lattice constant was fixed at $a=4.05$ Å. The numbers in parentheses in the first column are the number of $\mathbf{k}$ points in the irreducible wedge.

$\mathbf{k}$ points in the BZ	$G^2_{\min}=5.0$ Ry, $G^2_{\max}=6.0$ Ry,		$G^2_{\min}=7.0$ Ry, $G^2_{\max}=9.0$ Ry	
	E_T	E_W	E_T	E_W
64 (8)	−4.1334	10.3	−4.1721	10.4
216 (16)	−4.1551	11.5	−4.1983	11.5
512 (29)	−4.1513	11.1	−4.1936	11.3
1000 (47)	−4.1504	11.0	−4.1926	11.3
1728 (72)	−4.1521	11.0	−4.1947	11.1

B. Forces

A thorough discussion and derivation of the atomic forces have been given by Yin and Cohen.[29] The total force acting on an atom s in the unit cell can be divided into two contributions: (i) The force $\mathbf{F}_c$ due to the other atomic cores, and (ii) the force $\mathbf{F}_e$ due to the electrons. The atomic-core contribution is as given in Ref. 29. An alternate simple derivation for the electron contribution to the force starts with the expectation value of the valence ionic pseudopotential

$$\langle V\rangle=\sum_{n,\mathbf{k}}\langle\Psi_{n,\mathbf{k}}(\mathbf{r})\,|\,\sum_{l}V_{\mathrm{L}}^{P}(\mathbf{r}-l-\tau_s)+\sum_{l}V_{\mathrm{NL}}^{P}(\mathbf{r}-l-\tau_s)\,|\,\Psi_{n,\mathbf{k}}(\mathbf{r})\rangle\ , \tag{1}$$

where l is the direct lattice vector, and τ_s the position vector of the atom s in the unit cell. The valence ionic-core pseudopotential is decomposed into local (V_{L}^{P}) and nonlocal contributions (V_{NL}^{P}). The summation is over all the occupied states in the first BZ. The Bloch wave function corresponding to the band (n) and the wave vector ($\mathbf{k}$) is given by

$$\Psi_{n,\mathbf{k}}(\mathbf{r})=\frac{1}{\sqrt{N\Omega}}\sum_{\mathbf{G}}a_n(\mathbf{k},\mathbf{G})\exp[i(\mathbf{k}+\mathbf{G})\cdot\mathbf{r}]\ , \tag{2}$$

where $\mathbf{G}$ is the reciprocal lattice vector, $N\Omega$ the total crystal volume, N the number of unit cells, and Ω the volume of the unit cell. Then, F_e is the negative gradient of Eq. (1) with respect to the position vector τ_s. By substituting Eq. (2) in Eq. (1), and taking gradient with respect to τ_s, for the force on atom s we obtain

$$\mathbf{F}_e^s=\frac{1}{V}\sum_{n,\mathbf{k}}\sum_{l}\sum_{\mathbf{G},\mathbf{G}'}a_n^*(\mathbf{k},\mathbf{G}')a_n(\mathbf{k},\mathbf{G})\left\{\int e^{-i(\mathbf{k}+\mathbf{G}')\cdot\mathbf{r}}[-\nabla_{\tau_s}V_{\mathrm{L}}^{P}(\mathbf{r}-l-\tau_s)]e^{i(\mathbf{k}+\mathbf{G})\cdot\mathbf{r}}d^3r+\int e^{-i(\mathbf{k}+\mathbf{G}')\cdot\mathbf{r}}[-\nabla_{\tau_s}V_{\mathrm{NL}}^{P}(\mathbf{r}-l-\tau_s)]e^{i(\mathbf{k}+\mathbf{G})\cdot\mathbf{r}}d^3r\right\}\ , \tag{3}$$

where we identify the first (second) term with the local (nonlocal) contribution to the valence-electron force. Equation (3) can be brought into the desired final form by (i) rewriting the integrand using the distributive property of the gradient operator, (ii) defining $\mathbf{r}'=\mathbf{r}-l-\tau_s$, (iii) using $\nabla_{\tau_s}=-\nabla_{\mathbf{r}}$, and (iv) also performing the l summation:

$$\mathbf{F}_e^s=i\Omega\sum_{\mathbf{G}}\mathbf{G}\rho^*(\mathbf{G})e^{-i\mathbf{G}\cdot\tau_s}V_{\mathrm{L}}^{P}(\mathbf{G})-i\sum_{n,\mathbf{k}}\sum_{\mathbf{G},\mathbf{G}'}a_n^*(\mathbf{k},\mathbf{G}')a_n(\mathbf{k},\mathbf{G})(\mathbf{G}-\mathbf{G}')\times e^{-i(\mathbf{G}'-\mathbf{G})\cdot\tau_s}V_{\mathrm{NL}}^{P}(\mathbf{k}+\mathbf{G}',\mathbf{k}+\mathbf{G})\ , \tag{4}$$

where the Fourier transforms are defined as

$$V_{\mathrm{L}}^{P}(\mathbf{G})=\frac{1}{\Omega}\int V_{L}^{P}(\mathbf{r})e^{-i\mathbf{G}\cdot\mathbf{r}}d^3r\ , \tag{5}$$

$$V_{\mathrm{NL}}^{P}(\mathbf{k}+\mathbf{G}',\mathbf{k}+\mathbf{G})=\frac{1}{\Omega}\int e^{-i(\mathbf{k}+\mathbf{G}')\cdot\mathbf{r}}V_{\mathrm{NL}}^{P}(\mathbf{r})\times e^{i(\mathbf{k}+\mathbf{G})\cdot\mathbf{r}}d^3r\ , \tag{6}$$

$$\rho(\mathbf{G}-\mathbf{G}')=\sum_{n,\mathbf{k}}a_n^*(\mathbf{k},\mathbf{G}')a_n(\mathbf{k},\mathbf{G})\ . \tag{7}$$

In the expression for the valence-electron contribution to the force in Eq. (4), we also used the fact that V_{NL}^{P} vanishes outside the atomic-core region.

C. 1D calculations

The local part of the self-consistent potential obtained from the slab calculations is averaged on the parallel (xy) planes closely spaced along the z axis, it being perpendicular to the surface. The resulting 1D potential, $\bar{V}(z)$, is reminiscent of the square-cut potential, but is more realistic for the following reasons: Primarily, since the SCF-slab potential has a small corrugation outside the surface the 1D potential is rather close to the realistic slab potential. Within the film, the discrete nature of the slab is taken into account at least along the z direction. Of even more importance, $\bar{V}(z)$, being the (xy) average of the slab potential, contains the electron screening. In this respect, it is also significantly different from the square-cut or Sommerfeld model,[10,11] since electrons confined in the Sommerfeld-model potential are assumed to be noninteracting. Thus all essential ingredients of the SCF-slab potential are included in the 1D potential generated in our present study. The wave functions of the electrons confined in the potential, $\bar{V}(z)$, are separable, and can thus be written as

$$\Phi_{n,\mathbf{k}_{\parallel}}(x,y,z)=\zeta e^{i\mathbf{k}_{\parallel}\cdot\mathbf{r}}\phi_n(z)\ , \tag{8}$$

where the wave vector $\mathbf{k}_{\parallel}$ is parallel to the surface, and $\mathbf{r}$ is the position vector. The bound states of $\phi_n(z)$ have $n-1$ nodes inside the well, but decay on the outside. With the total wave function in Eq. (8), the 3D Schrödinger equation reduces to the following 1D form in atomic units:

$$\left[-\frac{d^2}{dz^2}+\bar{V}(z)\right]\phi_n(z)=\epsilon_n\phi_n(z)\ , \tag{9}$$

where ϵ_n is the energy of the subband. By adding the energy associated with the free-electron part in the (xy) plane, we obtain the one-electron energy $E_{n,k_{\parallel}}=k_{\parallel}^2+\epsilon_n$. Since $\bar{V}(z)$ is expressed on a grid consisting of n points on the z axis, the 1D Schrödinger equation is converted to a

system of n-linear equations, and solved numerically by diagonalizing the matrix constructed therefrom.[16,30] The charge density of the quasi-two-dimensional system[9,31] under consideration is given by

$$\rho(z)=D_2\sum_n (E_F-\epsilon_n)\,|\,\phi_n(z)\,|^2\,. \tag{10}$$

Here, E_F denotes the Fermi energy of the N-electron system confined in the well, and $D_2=m/\pi\hbar^2$ is the state density of the 2D noninteracting electron gas which is independent of energy and simply $1/2\pi$ in atomic units. From Eq. (10), a relation between E_F and the 2D charge density ρ_s [i.e., number of confined electrons per unit area of (xy) plane] is deduced:

$$\rho_s=D_2\sum_n (E_F-\epsilon_n)\,. \tag{11}$$

The density of states of a quasi-two-dimensional system, studied here by using the potential $\overline{V}(z)$, is given by

$$D_{2q}(E)=\sum_n \Theta(E-\epsilon_n)D_2 \tag{12}$$

and because of the step function $\Theta(E)$ is ladder-type in form. Accordingly, whenever a subband ϵ_n falls below the Fermi level, $D_{2q}(E_F)$ increases by a step of D_2. As the next section shows, this property of the quasi-two-dimensional system has important implications for the electronic properties.

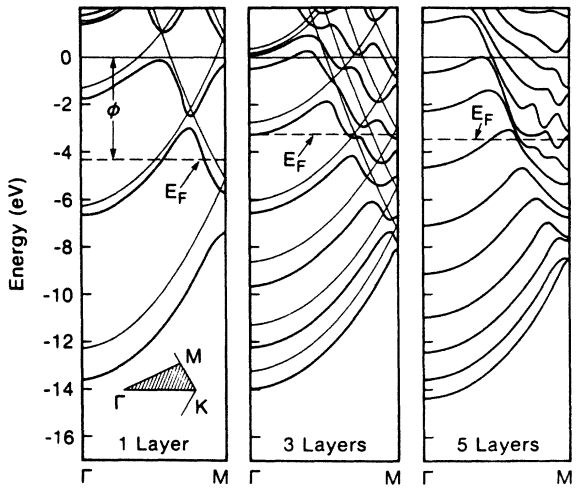

FIG. 1. Energy-band structures of one, three, and five layers of aluminum calculated using the self-consistent pseudopotential method are shown by thick lines. Thinner lines correspond to subbands obtained from the quasi-two-dimensional system quantum-well structure. (To avoid confusion, thinner lines of five-layer aluminum are not shown.) Energy is measured with respect to vacuum level. The inset shows symmetry directions of the surface Brillouin zone (after Ref. 16).

III. ELECTRONIC PROPERTIES AND ENERGETICS

The energy band structure of one, three, and five layers of Al films are calculated self-consistently along the ΓM direction of the surface BZ, and illustrated in Fig. 1. Since the lattice parameters of the monolayer undergo a significant contraction ($\sim$7%), results for the monolayer are obtained from the optimized geometry. As for multiple-layer films, lattice contraction and vertical surface relaxation are not sufficiently significant to essentially affect our conclusion regarding the electronic properties, therefore, ideal geometries of the multilayer films are used. We shall return to the oscillatory surface relaxations in Sec. V. The potential $\overline{V}(z)$ of the one- and three-layer Al films was described in Sec. II. The 1D potential and the electronic energy structure calculated therefrom are shown in Figs. 2 and 3. The subbands $E_{n,k_{||}}=\epsilon_n+k_{||}^2$, corresponding to each eigenvalue ϵ_n obtained from the solution of the 1D Schrödinger equation, are displayed

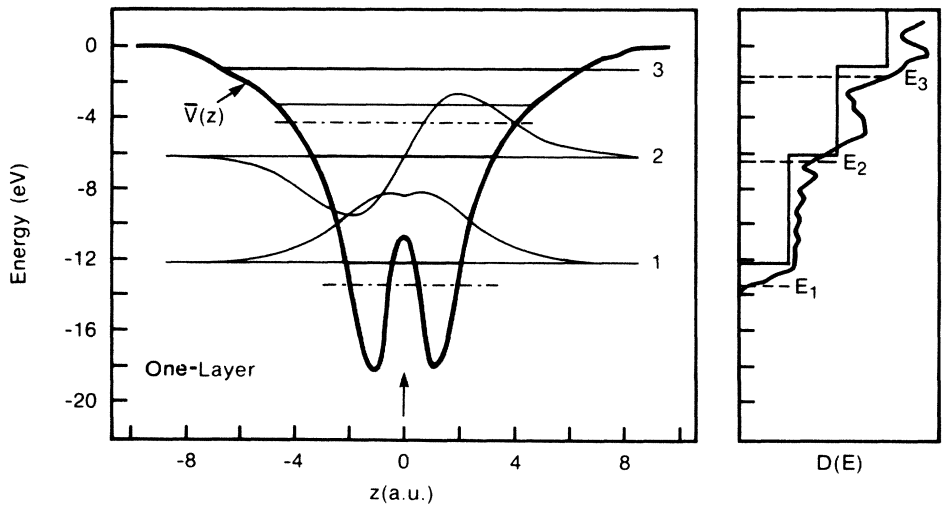

FIG. 2. 1D potential (quantum well) generated by the planar average of the self-consistent slab pseudopotential calculated for an unsupported Al monolayer. Energy levels and wave functions shown by 1 and 2 are the occupied subbands. Conduction band and energies at $\mathbf{k}=0$ of the slabs are indicated by dashed-dotted and dashed lines, respectively. The ladder-type state densities of the quasi-two-dimensional system, and the density of states of slabs calculated using 144 $\mathbf{k}$ points are shown in the right-hand panel. Energies are measured with respect to the vacuum zero. The atomic plane located at $z=0$ is indicated by an arrow (after Ref. 16).

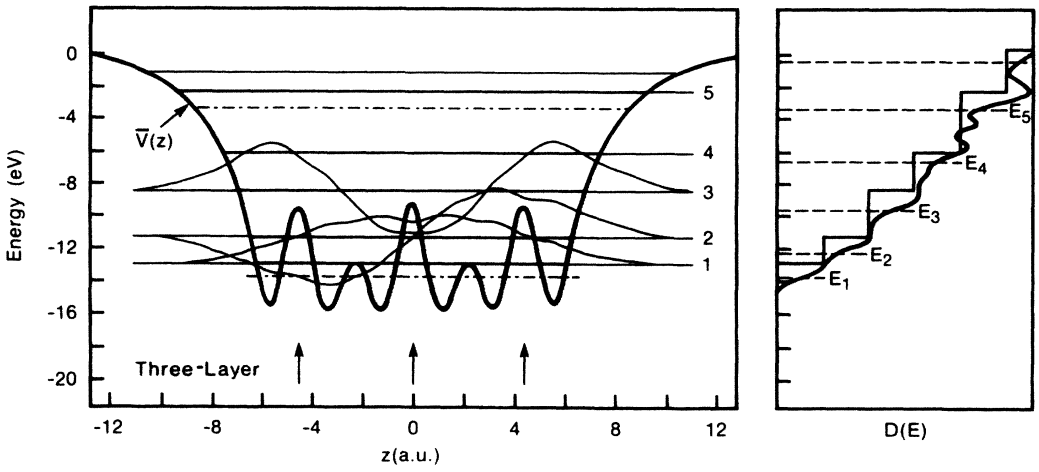

FIG. 3. The 1D potential (quantum well) generated by a planar average of the self-consistent slab pseudopotential calculated for a three-layer Al slab, and the electronic structure obtained from this potential. For further explanation of this figure, see the caption for Fig. 2 (after Ref. 16).

along with the self-consistent slab bands in Fig. 1. Also shown are Fermi-level E_F and work function Φ, in each case. As seen clearly, the slab bands and the subbands of the quasi-two-dimensional system follow one another closely, except that the former splits at the zone face because of the (xy) corrugation of the potential. Comparing the two sets of bands demonstrates that the thin Al film does indeed have a quasi-two-dimensional character with $m_x^* = m_y^* \approx m$. Since the nonlocal part in the planarly averaged potential is absent, the subbands, $E_{n,k}$ and the Fermi level of the quasi-two-dimensional systems described in Figs. 2 and 3 are shifted upwards relative to those calculated for the 3D slab. However, this simple model can suitably locate the Fermi level with respect to empty and occupied subbands. Moreover, for reasons previously pointed out, the 1D potential obtained by a planar average of the SCF pseudopotential is capable of providing a more realistic description of the s-p bonded metal film than a simple square-cut potential or the jellium model. Simple models, such as the square-cut potential or infinite potential well, give the subband spacings $(E_{n+1} - E_n)$ as being proportional to $(2n+1)/L^2$, where noninteracting electrons are confined in length L along the z direction. On the other hand, a planarly averaged potential as used in this study yields a quantization quite different from the $(2n+1)/L^2$ quantization, and close to that obtained from the slab calculations in Fig. 1. This can be seen from the irregular spacing of energy levels at the Γ point.

In accordance with Eq. (12), the density of states calculated for the quasi-two-dimensional system displays a ladder-type structure in Figs. 2 and 3, where the state densities of the one- and three-layer Al films calculated by the SCF-pseudopotential method are superimposed. Except for some additional structure owing to corrugation of the potential perpendicular to the z axis, the densities of states of slabs are also ladder shaped indicating the dimensionality of the metal films. As the number of layers increases, the step density per energy unit augments, and eventually the system becomes three dimensional. It should be noted that in the limit of large L, the state density corresponding to an infinite potential well changes from the ladder type to the parabolic form of a free electron gas ($\sim E^{1/2}$). In a real metal film, the values of the subband energies at Γ, i.e., ϵ_n, are closely related to the form of the planarly averaged potential. Consequently, as the metal film becomes thicker the density of states $D_3(E)$ deviates from the $(E^{1/2})$ relation characteristic of the 3D noninteracting free-electron system. In Fig. 4, the layer densities of states and the total densities of states calculated for the three-layer Al slab are illustrated. Also

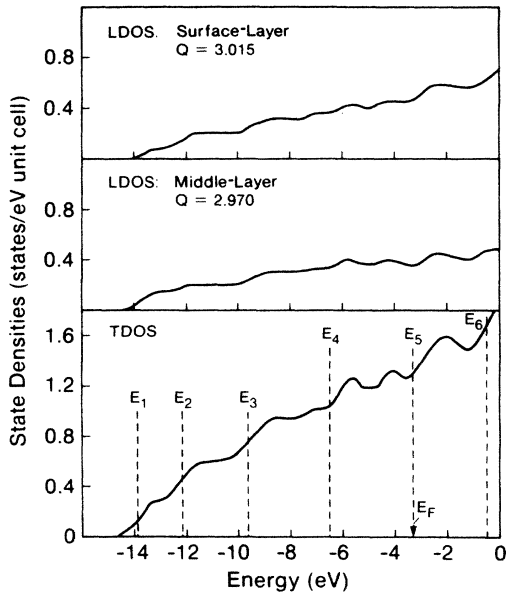

FIG. 4. Layer and total densities of states calculated for a three-layer slab by using the self-consistent pseudopotential method. Subband energies at $k=0$ (E_1, E_2, etc.) are indicated by dashed lines. Q is the charge per unit cell of a layer in units of electron. Zero of energy is set at the vacuum level.

shown are the subband energies at the Γ point. The jump of the density of states at the band energies is easily discernible. Because of a rather crude sampling grid in the surface BZ, the jumps are not as sharp as in the quasi-two-dimensional system. The electronic charge of the outermost layer is larger than the middle layer, implying that charge is transferred to the surface. Since the calculation is performed by partitioning space (for which no rigorous criterion is known), the charge-transfer values are only to be viewed qualitatively.

The confinement length of the electrons being finite in a thin metal film, crossing of the Fermi level by an empty subband owing to the increase of L gives rise to a jump in the density of states near the Fermi level. This sudden increase in the state density is certainly negligible for a thick film, but causes significant changes in the electronic properties as the metal film becomes thinner. For example, as revealed in the present study, work function Φ, and the surface energy exhibit fluctuations with varying thickness of the metal film. Certainly these fluctuations are damped with increasing thickness, and eventually saturate for thick films. In the jellium model, an additional subband drops below the Fermi level whenever L increases by half the Fermi wavelength. Since the positively charged atomic cores are smeared out, and thus the discrete lattice nature is omitted in the jellium model, the confinement length L can be increased continuously. As a result, the oscillatory character of the work function is easily obtainable. The work function, surface energy, and conduction-band width of the Al films with varying thicknesses are calculated by the SCF-pseudopotential method and listed in Table II. The work function of the monolayer is large and close to that of the semifinite slab ($\sim$4.3 eV). On going to the three-layer slab, it decreases to 3.2 eV and thus passes through a minimum. In the five-layer slab, Φ again increases to 3.4 eV and reaches a value of 3.7 eV in the seven-layer slab.

In this study, the total energy per atom is calculated for both the thin film and the bulk metal. By definition, the surface energy per surface atom, E_s, is one half (because of two surfaces) the difference between the slab and bulk total energy for the same number of atoms as in a slab, i.e., $E_s = (E_T, \text{slab} - E_T, \text{bulk})/2$. As seen in Table II, the surface energy of a metal film is another property which exhibits oscillatory behavior as the film thickness varies. It is low in a monolayer, but increases and passes through a maximum in the three-layer film, and decreases again for five- and seven-layer Al films. The trend of the surface energy is opposite to that of the work function, which passes through a minimum for the three-layer Al film.

The conduction-band width also undergoes a change when the metal film becomes very thin. For a monolayer, it is only 9.1 eV, but increases with the increasing number of layers, and saturates at about five layers. A straightforward expectation along the trends seen in the work function and surface energy would be an oscillatory variation of the conduction-band width as the thickness varies. However, the number of nearest neighbors is the most relevant parameter in determining the width, so the variations induced by the size effect are overshadowed. Oscillations of the work function and surface energy have a close connection to the changes of the surface charge density; it is discussed in the following sections.

IV. CHARGE-DENSITY ANALYSIS

Distribution of the surface charge and thus the dipole moment originating therefrom are expected to influence the properties of thin metal films. Here, we give a detailed analysis of the charge density obtained from SCF-pseudopotential calculations. In Fig. 5, we present the contours of the total charge density on an (xy) plane passing through the surface atoms of the Al films for three different films (one, three, and five layers). Among all the slabs considered, the monolayer has the highest charge density which occurs at the center of the line joining the nearest-neighbor atoms. In a shell around an atom in a monolayer, the charge density does not show any significant variations ($\sim$0.001 a.u.) and thus the constant density contours are almost circular. For a three-layer film, there are two maxima on the line connecting two nearest neighbors, and a shallow minimum at the center of the equilateral triangles (formed by three nearest-neighbor atoms). The difference between the maximum and minimum charge densities is larger than for the monolayer case. In the five-layer Al film, the charge density in the interatomic region becomes structureless except for a shallow minimum at the center of the equilateral triangles having vertices at the atoms. The fcc close-packed stacking, underlies the variations in the structure of the charge density. The two halves of the surface unit cell show only a slight difference. In Fig. 6, the contour plots of the charge density in an (xz) plane perpendicular to the surface are shown. The charge density above the surface of the monolayer Al is higher and displays less corrugation than that of the three-layer Al. Figure 7 shows the (xy)-planarly averaged charge density, $\bar{\rho}(z)$, of the one-, three-, and five-layer Al films plotted along the z axis pointing towards the vacuum. It is clearly seen that the monolayer has the highest charge density in a region extending from

TABLE II. Work function Φ (eV), surface energy E_s (eV per surface atom), and bandwidth E_W (eV) calculated for one, three, five, and seven layers of aluminum thin film. The values in parentheses correspond to the ideal monolayer.

	One layer	Three layer	Five layer	Seven layer
Φ	4.3 (4.12)	3.2	3.4	3.7
E_s	0.42 (0.47)	0.50	0.49	0.44
E_W	9.1 (7.8)	10.5	10.9	10.9

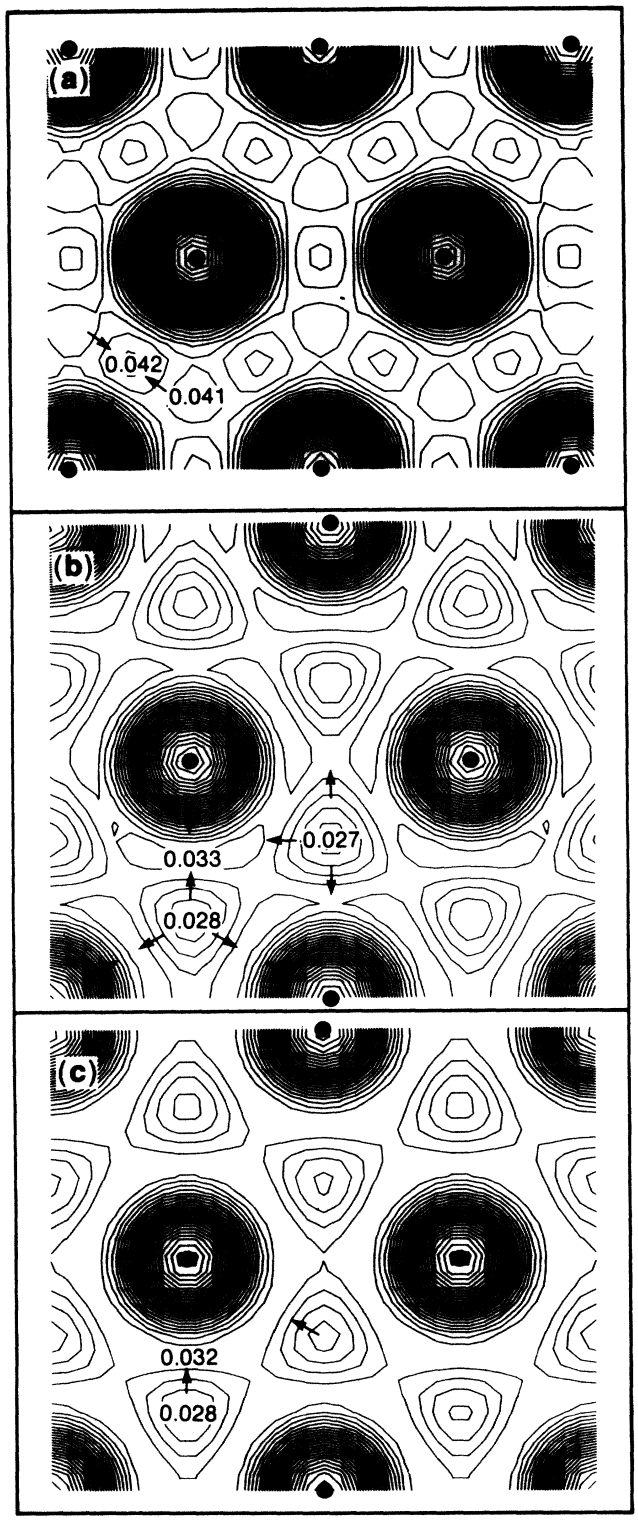

FIG. 5. Charge-density contours in the outermost atomic (111) plane of (a) one-layer, (b) three-layer, and (c) five-layer Al films. Solid circles indicate the position of aluminum atoms. Charge density increases in the directions of small arrows. The contour spacings are 0.0012 a.u. The values of the charge density at certain locations are given.

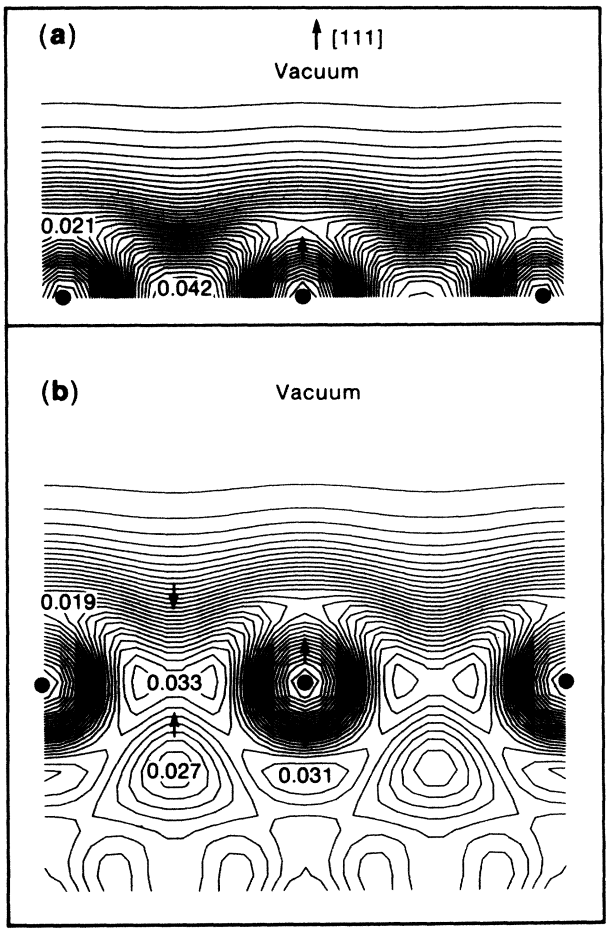

FIG. 6. Charge-density contours in a vertical plane calculated for one- and three-layer Al films. For further explanation see Fig. 5.

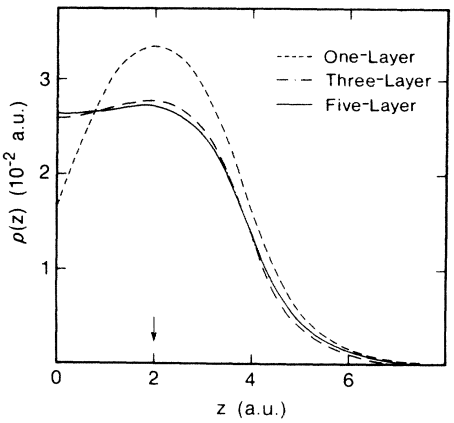

FIG. 7. The (xy) averaged charge density calculated for one-, three-, and five-layer Al(111) films by using the self-consistent pseudopotential method. The outermost atomic planes are located at $z=2$ a.u. indicated by an arrow. The surface normal is along the z axis and points outwards.

the atomic plane to the vacuum. Comparison of three- and five-layer films reveals that the average charge density of the three-layer at the outermost atomic plane is higher than that of the five-layer Al film, except, in a region extending from 2 a.u. above the surface towards vacuum. Near the surface region for $z<0$, $\bar{\rho}(z)$ displays small Friedel oscillations which is appropriate for Al. Fluctuations of the surface charge density as a function of film thickness have important implications for the electronic properties as discussed in Sec. VI.

V. SURFACE RELAXATIONS

In the last decade, experimental data from LEED experiments have shown that the clean metal surfaces are subject to reconstruction or relaxation.[32] Such changes in the geometry of the surfaces can have significant effects on the properties of metals. Atoms near the surface of a metal are under the influence of forces different from those of the bulk, and which are known to lead to multilayer relaxations.

Low-energy electron diffraction data from aluminum low-index surfaces have been interpreted to indicate an inward relaxation, i.e., a contraction of 10—15% in the spacing of the (110) surface layer from the first sublayer compared with the bulk.[33–35] On the (111) and (100) surfaces, no such contraction was found within an accuracy of 5%.[35] Using a uniform charge-density model, Finnis and Heine[36] have presented a simple explanation for contraction of the surface-layer spacing within the single-layer relaxation approach. Moreover, their simple theory revealed that contraction of the close-packed (111) surface is smaller than for open surfaces. Later, Landman *et al.*[37] predicted an alternating change in sign of the multilayer relaxation in the first few surface layers, confirmed by the extensive LEED analysis on the Al(110) surface. Experiments by high-energy ion scattering[38] have also shown oscillatory relaxation on the Al(110) surface. Experimental data on relaxation of the Al(111) surface seem to be at variance: For example, the first interlayer spacing expands by 2% according to LEED measurements,[39] which appears to be in contradiction to predictions by Finnis and Heine,[36] whereas the extended x-ray-absorption fine structure data[40] indicates an 8% contraction. In spite of these controversial results, common belief is that the surface relaxation recedes as the atomic density of the planes increases, and thus becomes insignificant for the Al(111) surface.[41] It is now well known that the charge density near the outermost plane is closely related to the force acting on this plane. As revealed from previous discussions, the surface charge density varies in turn as a function of film thickness causing fluctuations in the electronic properties. Consequently, surface relaxation is expected to exhibit similar behavior, i.e., a size effect.

We now focus our attention on the direction rather than on the magnitude of the oscillatory multilayer surface relaxations of the thin Al films. Accordingly, we have calculated forces exerted on the (111) atomic planes, and deduced the direction of relaxation. Forces were calculated on the three-, five-, and seven-layer Al(111) slabs in their ideal atomic configurations, and results are listed in Table III. The force exerted on the surface plane of the three-layer Al film is directed inwards towards the center of the slab, and thus indicates inward relaxation or contraction of the interlayer spacing. In the five-layer Al film, two interlayer spacings are subject to change. The direction of the forces calculated yields a contraction of the first-interlayer spacing, i.e., inward relaxation of the surface plane, and a small expansion of the second-interlayer spacing (i.e., spacing between the second and third layers below the surface plane). As revealed earlier,[42] the forces calculated correlate quite well with equilibrium relaxations, and can thus be used as a measure for changes in interlayer spacings. On the basis of this argument, one may conclude that contraction of the first-interlayer spacing is enhanced in the five-layer film. It is interesting to note that the first-interlayer spacing of the seven-layer Al film expands. In percentage, the change in the first-interlayer spacing is smaller than those of the three- and five-layer films, and is obviously in the opposite direction. The second-interlayer spacing undergoes a contraction, and the third-interlayer spacing again expands. The underlying physics in the oscillatory relaxation has been extensively discussed in previous studies, and in agreement with those arguments the directions of the forces calculated result in oscillatory multilayer relaxation. In the present study, the new result is the change in sign of the first-interlayer spacing as a function of film thickness. In view of the distribution of the electronic energy states, it has been argued that Al films from monolayer up to five-layer thickness reflect the properties of a 2D electron system, and 3D characters start to appear from a seven-layer film. Therefore, expansion of the first-interlayer spacing obtained in the seven layer, which is in qualitative agreement with LEED measurements on the Al(111) surface, strengthens our arguments about the dimensionality of the metal film. Recent calculations by Ho and Bohnen[42] have yielded small fluctuations in the relaxation of the Al(110) slabs as the thickness is increased from 9 to 15 layers. They attributed these small fluctuations to interactions between the two surfaces of the slab rather than to a size effect. They pointed out that the slab must be at least 13 layers thick to yield reasonably converged results. It is known that the (110) surface plane of aluminum relaxes toward the second surface layer, and therefore the size effect beyond nine layers appears as a small fluctuation above the value of the contraction. Since the first-interlayer spacing of the (111) surface of thick aluminum undergoes a small expansion, the size effect seems to change the qualitative

TABLE III. Calculated forces on atomic planes in the ideal geometry. Positive and negative values indicate forces directed outwards and inwards, respectively.

	Force (m Ry/a.u.)		
Plane	Three layer	Five layer	Seven layer
1	−17.8	−18.2	−4.2
2	0.0	0.9	−9.0
3		0.0	7.6
4			0.0

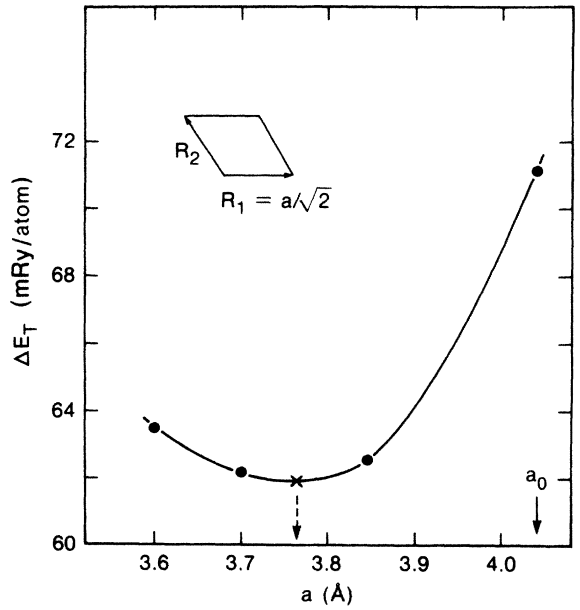

FIG. 8. The total-energy difference between the Al(111) monolayer and bulk aluminum as a function of lattice parameter a. The inset shows the surface unit cell and primitive translation vectors $\mathbf{R}_1$ and $\mathbf{R}_2$ of length $a/\sqrt{2}$. The equilibrium lattice parameters of bulk Al, a_0, is also indicated.

character of the surface relaxation so that it turns to contractions at very thin films.

Lateral relaxation, i.e., uniform change of the 2D lattice parameters is not conceivable for thick films, but as pointed out earlier by Batra[28] becomes important for an unsupported metal monolayer. To investigate the lateral relaxation of the Al(111) monolayer, we carried out total-energy calculations to determine the equilibrium lattice parameter. Figure 8 shows the change of the total energy per atom of the Al monolayer as a function of the lattice parameter. It is noted that the Al monolayer has an equilibrium lattice constant 7% smaller than the ideal bulk value. The underlying physics of this contraction can be seen in the number of nearest-neighbor atoms. In the bulk, each Al atom is surrounded by 12 Al atoms, whereas the number of nearest neighbors in the monolayer reduces to six, which is expected to influence the charge distribution and various properties connected with it. In Table IV, variations of the total energy and bandwidth as a function of lattice parameter are listed. The bandwidth (measured from the first subband up to E_F) increases by 17%. It is interesting that change of the bandwidth as a function of lattice parameter follows the d^{-2} rule proposed by Harrison and Ciraci.[43] Many properties of thin metal films are known to be correlated by the average charge density. In the monolayer, lattice contraction imposes a change $\sim 18\%$ in 2D charge density ρ_s, and a 4% increase in the work function.

TABLE IV. Total energy E_T,E_T minus the total energy per atom of bulk aluminum, ΔE_T; the width of the valence band E_W calculated for the Al(111) monolayer with different lattice parameters.

a (Å)	E_T (Ry)	ΔE_T (Ry)	E_W (eV)
4.05	−4.1234	0.0713	7.8
3.85	−4.1323	0.0625	8.4
3.70	−4.1324	0.0623	9.0
3.60	−4.1312	0.0635	9.5

VI. DISCUSSIONS: QUANTUM SIZE EFFECT

The results presented in the preceding sections clearly demonstrate that several properties of thin Al films (such as work function, surface energy, bandwidth, surface relaxation, and charge density in the surface region) are strongly dependent on film thickness. For example, values of work function, surface energy, and vertical relaxation of the surface vary with thickness. These fluctuations will saturate to values of the semi-infinite slab by damped oscillations. Figure 9 shows variations of the work function, surface energy, etc. The oscillatory behavior of the electronic properties, especially that of the work function is closely related to the surface electronic-charge distribution varying as a function of film thickness.[13] Once the number of metal layers increases, which results in an empty subband (contributing to the surface charge much more than the lower-lying states in Figs. 2 and 3) dipping below the Fermi level, the surface charge starts to increase. The surface-charge density passes through a local maximum at the Fermi-level position near the midpoint between the occupied and next empty sub-

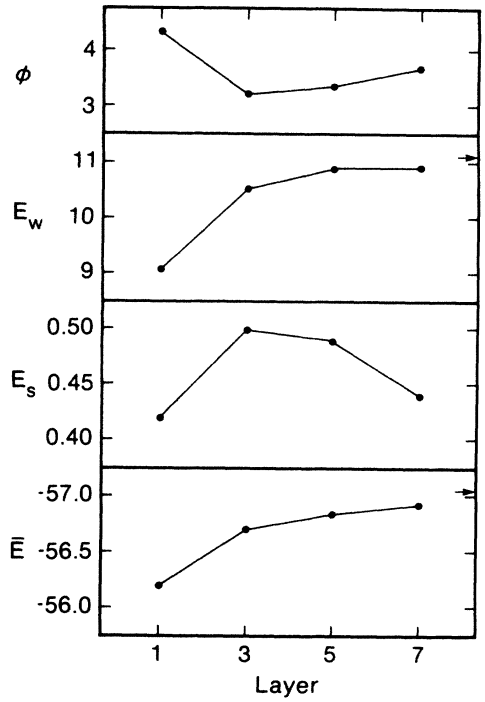

FIG. 9. Work function Φ (eV), conduction bandwidth, E_W (eV); surface energy, E_s (eV per surface atom) and average total energy $\bar{E}$ (eV per atom) of one-, three-, five-, and seven-layer Al(111) films. The values of even-numbered layers are not shown. Calculated values are joined by straight lines. Small arrows show values corresponding to bulk Al.

bands. Further increase of the film thickness causes the next empty subband to become close to the Fermi level, and the surface charge to recede because of the dominating effect of the enlarged length of confinement. Consequently, the surface dipole moment, and thus the work function, is near a local minimum wherever the Fermi level becomes closer to a subband. This assertion can be easily verified by comparing Figs. 7 and 10. The Fermi level of the monolayer is located at the middle of subbands $n=2$ and 3, and has highest charge density above the surface. Consequently, it has the largest work function. On going to the three-layer Al film, subband $n=3$ falls far below the Fermi level, and subband $n=4$ is very close to it. According to the above arguments, this position of the Fermi level corresponds to a local minimum of the surface-charge density. It is generally expected that the larger the charge depletion from the slab (or conversely the larger the charge spilling above the surface), the higher the surface dipole moment. The work function associated with the surface is proportional to the value of the dipole moment. Thus, as expected, the work function of the three-layer Al film is decreased. However, the position of the Fermi level of the five-layer Al is quite different from the three-layer Al, but similar to that of the monolayer, where E_F lies between subbands 7 and 8. Accordingly, the charge density above the surface exceeds that of the three-layer film (see Fig. 7) and the work function is increased. In Fig. 10, an interesting situation arises regarding the position of the Fermi level of the seven-layer Al film: The work function is larger than that of the five-layer film in spite of the Fermi level being close to subband $n=10$. This implies that the work function passes through a local maximum at a six-layer Al film. Comparing variation of the work function and surface energy in Fig. 9, one observes that the surface energy exhibits a reverse trend. It is low in the monolayer, but passes through a maximum for a three-layer film. Further increase of the thickness up to seven-layer causes the surface energy to decrease. It is noted that the work-function values quoted do not include small corrections[42] owing to nonzero charge density [$\sim 10^{-6}$ electrons/(a.u.)^3] in the middle of the vacuum region.

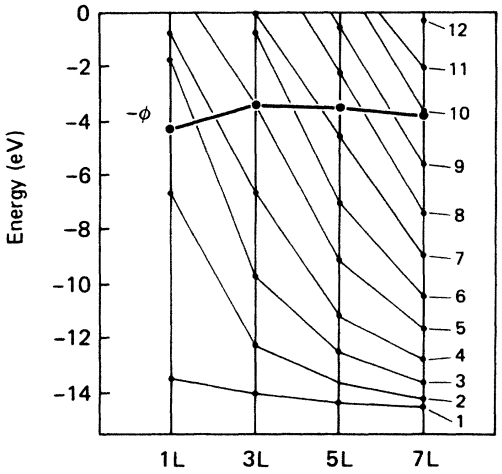

FIG. 10. Work function and subband energies (at Γ) of one, three, five, and seven layers of Al(111) thin films calculated by the self-consistent pseudopotential method. Even-numbered layers are not shown. To highlight the changes, values of work function and subband energies are joined by thick and thin straight lines, respectively (after Ref. 16).

A comment on the effect of the surface relaxation on the work-function values is in order. As pointed out in Sec. III, except for lateral relaxation of the monolayer, the work function of multilayer films was calculated from the slabs with ideal lattice parameters. While the calculated forces on the atoms indicate multilayer vertical relaxations, the values of these relaxations are known to be small for the Al(111) surface. Ho and Bohnen[42] found a small change in work function of ~ 0.2 eV between relaxed and ideal Al(110) slabs. Since surface relaxation of the Al(111) slab is smaller than that of the Al(110) slab, the effect of surface relaxation on work-function values is expected to be negligible. Feibelman[15] carried out the total-energy minimization by allowing only the topmost layer to relax. His results show an expansion of the outermost-interlayer spacing, $\sim 6\%$ for two-layer and $\approx 4\%$ for six-layer films. In spite of outward relaxation of the surface layer, Feibelman[15] also found small variation on the work function upon surface relaxation. As for surface energy, the energy associated with multilayer relaxation was found to be ~ 10 meV for Al(110) slabs, which is only a small fraction of surface energy. As a result, the effect of surface relaxation on surface energies calculated for ideal Al(111) films is expected to be rather small.

The type of surface relaxation suggested in our work seems to be at variance with those found by Feibelman.[15] The forces exerted on the surface atoms suggest contraction of the interlayer spacing between surface and subsurface layers, and also oscillatory multilayer relaxation for three- and five-layer Al films. In the seven-layer Al film, the surface-layer plane exhibits very small inward relaxation. The magnitude of the forces indicates that inward relaxation of the surface sublayer is larger and thus leads to expansion of the first-interlayer spacing. Using a single-layer relaxation approach, Feibelman predicted the expansion of the first surface-interlayer spacing for thin Al(111) films consisting of two to six layers, in which the amount of expansion decreases as film thickness increases. The origin of the difference may lie in the fact that Feibelman allowed only the surface layer to relax leaving subsurface layers to preserve their ideal locations. As the present results show, surface relaxations in the three- and five-layer Al(111) films are rather different from those of seven-layer Al films. The first-interlayer spacing of the seven-layer Al films expands as (in fact) observed in semi-infinite slabs. This finding is consistent with our previous arguments stating that 3D properties start to appear in seven-layer film. Variation of surface energy as a function of thickness displays an inverse trend as compared to that of the work function, inasmuch as the surface energy retains the maximum values for a three-layer film, when the work function has minimum value. The theory of simple metals within local density-functional theory[14] and jellium approximation[44] showed that the sur-

face energy is closely related to distribution of the electronic charge density above the surface.

On the basis of the formalism presented in Sec. II, the position of the Fermi level has a close relationship to the 2D charge density ρ_s and also the potential of the quasi-two-dimensional system. Therefore, the exotic physical properties of very thin metal overlayers deposited on semiconductors can be related to the form of this interface potential, and thus to subband structure. When the form of this potential is changed by the substrate weakly interacting with the metal overlayer, $D_{2q}(E_F)$ may undergo a sudden change with significantly altered electronic properties. Evidently, such an effect cannot be deduced from simple quantization models.

Apart from subband structure, transfer of charge between metal overlayer and substrate causes surface-charge density ρ_s to undergo a change, which in turn affects the position of the Fermi level. Recently, Batra and Ciraci[45] have studied the Al overlayer on Ge substrate, and pointed out interesting size effects regarding thickness of the overlayer.

Finally, we should like to comment on two closely related concepts, interchangeably used, but which sometimes have quite different meanings. The above discussion clarifies that the 2D character is attributed to the thin Al films because of the character of the wave function. As such, the wave function has a free-electron solution in the (xy) plane, whereas it is confined in the potential well along the z axis. Several properties of thin films quite different from those of the bulk originate from the way one-electron states are quantized, and are related to the dimensionality of the system. However, the properties of three- and five-layer Al vary, in spite of the fact that both films have 2D character. These changes are associated with the different sizes of the thin films.

In conclusion, the relative position of the Fermi level with respect to the highest-occupied and empty subbands undergoes a change depending on the size of the film, which in turn influences surface-charge distribution and the resultant electronic properties. The relative position of the Fermi level between two subbands is also an important parameter in assessing properties of metal overlayers on semiconductor substrates. The density of states of a quasi-two-dimensional system is ladder shaped which can be taken as a fingerprint of dimensionality much like plasmon dispersion.[46–48]

ACKNOWLEDGMENTS

One of us (S.C.) would like to thank the IBM Almaden Research Center, where part of the work was performed, for their hospitality and support. We thank Dr. K. Kunc, Dr. K. M. Ho, and Dr. K. P. Bohnen for useful discussions.

---

*Permanent address: IBM Almaden Research Center, Mail Stop K33/801, 650 Harry Road, San Jose, CA 95120-6099.

†Permanent address: Middle East Technical University, Ankara, Turkey.

‡Permanent address: Physics Department, University of Ulster, Northern Ireland, BT 52 1SA, U.K.

§Permanet address: Department of Physics, University of California, Davis, CA 95616.

[1]J. A. Appelbaum and D. R. Hamann, Rev. Mod. Phys. **48**, 480 (1976).

[2]R. C. Jaklevic, J. Lambe, M. Mikkor, and W. C. Vassell, Phys. Rev. Lett. **26**, 881 (1971).

[3]A. Paskin and A. D. Singh, Phys. Rev. **140**, A1965 (1965).

[4]B. R. Cooper, Phys. Rev. Lett. **30**, 1316 (1973).

[5]P. Chaudhari, H.-U. Habermeier, and S. Maekawa, Phys. Rev. Lett. **55**, 430 (1985).

[6]I. P. Batra and S. Ciraci, Phys. Rev. B **12**, 6419 (1984).

[7]M. J. Burns, J. R. Lince, R. S. Williams, and P. M. Chaikin, Solid State Commun. **51**, 865 (1984).

[8]For an extensive discussion of the 2D electron system, see, for example, T. Ando, B. A. Fowler, and F. Stern, Rev. Mod. Phys. **54**, 437 (1982).

[9]R. Dingle, *Festkörperprobleme,* edited by H. J. Queisser (Pergamon, Oxford, 1975), Vol. XV, p. 21.

[10]B. G. Smith, Phys. Lett. **18**, 210 (1965).

[11]R. Stratton, Phys. Lett. **13**, 556 (1965).

[12]The quantum size effect of using the Schockley method of a 1D lattice was discussed in A. A. Cottey, J. Phys. C **6**, 2446 (1973), and references cited therein.

[13]F. K. Schulte, Surf. Sci. **55**, 427 (1976).

[14]P. Hohenberg and W. Kohn, Phys. Rev. **136**, B864 (1964); W. Kohn and L. Sham, Phys. Rev. **140**, A1133 (1965).

[15]P. J. Feibelman, Phys. Rev. B **27**, 1991 (1983).

[16]S. Ciraci, and I. P. Batra, Phys. Rev. B **33**, 4294 (1986).

[17]Ed. Caruthers, L. Kleinman, and G. P. Alldredge, Phys. Rev. B **9**, 3330 (1974); K. Mednick and L. Kleinman, *ibid.* **22**, 5768 (1980).

[18]J. R. Chelikowsky, M. Schlüter, S. G. Louie, and M. L. Cohen, Solid State Commun. **17**, 1103 (1975).

[19]I. P. Batra and S. Ciraci, Phys. Rev. Lett. **39**, 774 (1977).

[20]An extensive review on the electronic properties of aluminum has recently been given by I. P. Batra and L. Kleinman, J. Electron Spectrosc. Relat. Phenom. **33**, 175 (1984).

[21]M. Schlüter, J. R. Chelikowsky, S. G. Louie, and M. L. Cohen, Phys. Rev. B **12**, 4200 (1975).

[22]K. C. Pandey, Phys. Rev. Lett. **49**, 223 (1982).

[23]J. Ihm, A. Zunger, and M. L. Cohen, Phys. Rev. C **12**, 4409 (1979).

[24]M. T. Yin and M. L. Cohen, Phys. Rev. Lett. **45**, 1004 (1980).

[25]C. B. Bachelet, D. R. Hamann, and M. Schlüter, Phys. Rev. B **26**, 4199 (1982). See also D. R. Hamann, M. Schlüter, and C. Chiang, Phys. Rev. Lett. **43**, 1494 (1979).

[26]D. M. Ceperley and B. J. Alder, Phys. Rev. Lett. **45**, 566 (1980).

[27]J. P. Perdew and A. Zunger, Phys. Rev. B **23**, 5048 (1981).

[28]I. P. Batra, J. Vac. Sci. Technol. **3**, 1603 (1985).

[29]M. T. Yin and M. L. Cohen, Phys. Rev. B **26**, 3259 (1982).

[30]S. Erkoç and S. Ciraci, Phys. Rev. B **34**, 4360 (1986).

[31]Here, the word "quasi" is used to indicate that the electron system is really 3D but has free-electron character in the (xy) plane.
[32]See, for example, *Proceedings of the First International Conference on the Structure of Surfaces, Berkeley, 1984,* edited by M. A. Van Hove, and S. Y. Tong (Springer, Berlin, 1985).
[33]G. E. Laramore and C. B. Duke, Phys. Rev. B **5**, 267 (1972).
[34]D. W. Jepsen, P. M. Marcus, and F. Jona, Phys. Rev. **6**, 3684 (1972).
[35]M. R. Martin and G. A. Somorjai, Phys. Rev. B **7**, 3607 (1973).
[36]M. W. Finnig and V. Heine, J. Phys. F **4**, L37 (1974).
[37]U. Landman, R. N. Hill, and M. Mostoller, Phys. Rev. B **21**, 448 (1980); R. N. Barrett, R. G. Berrera, C. L. Cleveland, and U. Landman, *ibid.* **28**, 1667 (1983).
[38]Y. Kuk and L. C. Feldman, Phys. Rev. B **30**, 5811 (1984).
[39]F. Jona, D. Sonderikkner, and P. M. Marcus, J. Phys. C **13**, L155 (1980).
[40]A. Bianconi and R. Z. Bachrach, Phys. Rev. Lett. **19**, 104 (1979).
[41]T. Halicioğlu, H. Ö. Pamuk, and S. Erkoç, Surf. Sci. **143**, 601 (1984).
[42]K. M. Ho and K. P. Bohnen, Phys. Rev. B **32**, 3446 (1985); and (private communication).
[43]W. A. Harrison and S. Ciraci, Phys. Rev. B **10**, 1516 (1974).
[44]See, for example, J. R. Smith, Phys. Rev. **181**, 522 (1969); N. D. Lang and W. Kohn, Phys. Rev. B **1**, 4555 (1970).
[45]I. P. Batra and S. Ciraci, Phys. Rev. B **33**, 4312 (1986).
[46]D. M. Newns, Phys. Rev. B **8**, 3304 (1970); D. M. Newns, Phys. Lett. **38A**, 341 (1972).
[47]T. Argua, H. Tochiara, and Y. Murata, Phys. Rev. Lett. **53**, 372 (1984).
[48]S. Ciraci and I. P. Batra, Phys. Rev. Lett. **56**, 877 (1986), and references therein.

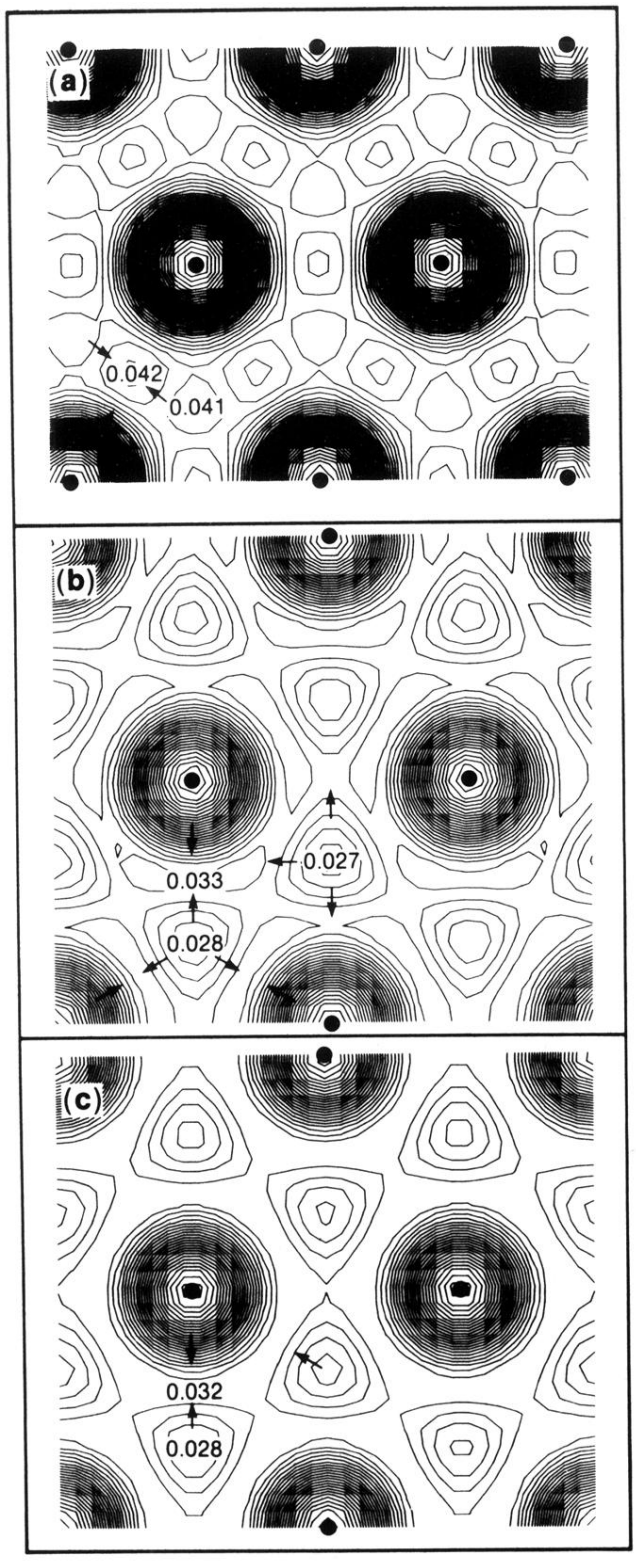

FIG. 5. Charge-density contours in the outermost atomic (111) plane of (a) one-layer, (b) three-layer, and (c) five-layer Al films. Solid circles indicate the position of aluminum atoms. Charge density increases in the directions of small arrows. The contour spacings are 0.0012 a.u. The values of the charge density at certain locations are given.

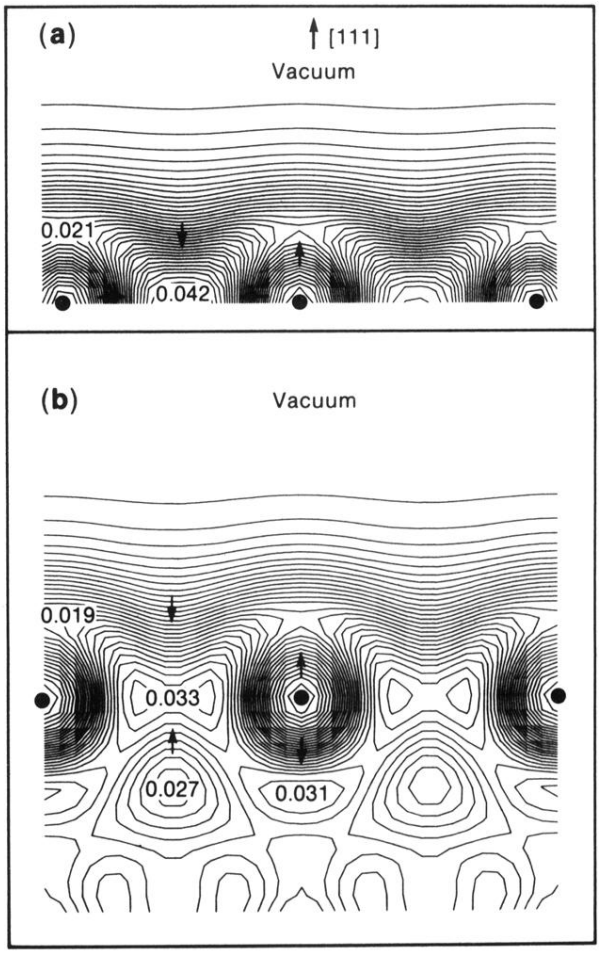

FIG. 6. Charge-density contours in a vertical plane calculated for one- and three-layer Al films. For further explanation see Fig. 5.